POLITECNICO DI TORINO
Repository ISTITUZIONALE

Strain-based method for fatigue failure analysis of truss lattice structures: modeling and experimental setup

Original
Strain-based method for fatigue failure analysis of truss lattice structures: modeling and experimental setup / Coluccia, A., DE PASQUALE, G.. - (2023), pp. 1190-1194. (17th European Conference on Spacecraft Structures Materials and Enviromental Testing Tolouse (FR) 28-30 Marzo 2023).

Availability:
This version is available at: 11583/2978388 since: 2023-05-08T12:13:36Z

Publisher:
Centre Nationale d'Etudes Spatiales

Published
DOI:

Terms of use:

This article is made available under terms and conditions as specified in the corresponding bibliographic description in the repository

Publisher copyright

(Article begins on next page)

10 November 2026

STRAIN-BASED METHOD FOR FATIGUE FAILURE ANALYSIS OF TRUSS LATTICE STRUCTURES: MODELING AND EXPERIMENTAL SETUP

Antonio Coluccia, Giorgio De Pasquale

Smart Structures and Systems Lab, Dept. of Mechanical and Aerospace Engineering, Politecnico di Torino, Corso Duca degli Abruzzi 24, Torino 10129, Italy.
e-mail: antonio.coluccia@polito.it, giorgio.depasquale@polito.it

KEYWORDS

Lattice structures, fatigue, finite elements method, lightweight, additive manufacturing.

ABSTRACT

Lattice structures, as a subclass of cellular solids, are nowadays among the most promising materials in lightweight engineering: their excellent mechanical properties, together with their functionality and reduced mass, make them the perfect candidates for many applications in the aerospace and automotive fields. Such sectors require though demanding specifications for their components: among all, fatigue behavior has high importance.
A simplified method for the fatigue analysis of lattice structures, based on finite element method (FEM) is proposed: through linear homogenization of the lattice structure, a lighter FEM model employed for the fatigue failure analysis is developed. Second step of the model is the application of de-homogenization on the most critical cell and therefore the recovery of the true state of the lattice. In this investigation, the method is employed in the case of a 4-point bending cyclic load, together with the presentation of a validating experimental setup.

1. INTRODUCTION

Properties of lattices structure have been widely investigated in the last years [1] [2] because of the advantages these materials can lead to. Main relevant aspect of lattices are of course their mechanical properties: not only they provide excellent strength and stiffness performances, but also these properties can be modulated and varied according to the structural specifications. This is partly due to additive manufacturing gifting lattices with a strong design freedom, with respect to conventional materials, that makes such structures employable in many fields of mechanics [3]. One of the most important fields where lattices are used is the aerospace: here, their functionality, and impact and energy absorption properties are investigated for different engineering solutions. In [4], lattices are used in the design of the leading edge of an aircraft wing: both their energy absorption properties and functionality are important, since the leading edge must resist to eventual impacts and accommodate the anti-icing system. Another interesting application for lattice-like structure can be found in [5], where repetitive unit metal composite panels are employed as spacecraft shields. Progressive failure of a lattice cylindrical panel meant for aerospace application under compression load can be found in [6].
Besides impacts and static loading, spacecraft structures need to be designed also taking into account fatigue failure: in [7], hexagonal honeycomb cores for space applications are tested under in-plane shear fatigue loading. Not only structures, but also instrumentation needs to be tested under vibrational fatigue conditions, as it can be seen in [8]. Fatigue is largely investigated in lattices as well: constant amplitude and random fatigue loading are considered in [9] for the characterization of an aluminum Schwartz periodic lattice structure, together with a detailed analysis of fracture surfaces. In [10], diamond and gyroid Ti6Al4V lattice structures are modeled via finite elements method (FEM) under compression low cycle fatigue loading; a similar investigation, but on the effect of load direction is conducted in [11]. A method to predict the fatigue life of a triangular cell lattice structure in presence of a pre-crack is proposed in [12], together with the experimental validation of the method.
While most methods for the analysis of fatigue failure of lattices are based on complex analytical models, often in combination with numerical FEM models, this investigation presents a simplified method that makes use of FEM for the homogenization and de-homogenization. Firstly, after selecting the topology of the cell to be employed, the lattice is homogenized: equivalent properties of a medium material representing the lattice as bulk material are extracted. The second step is the FEM analysis of the component, sample, or part, where the medium material is employed in place of the lattice. Once performed the analysis, the most critical lattice section is detected through a strain-based criterion. Then, the

de-homogenization is applied. In this way, it is possible to retrieve the true stress condition of the lattice cell and to apply a suitable fatigue failure criterion. In this paper, the method is applied in the case of a 4-points bending test; also, an experimental setup for the validation is presented. In a previous investigation [13], the method has been used in the case of a cantilever beam bending load application.

2. METHOD

An innovative sample configuration is presented for the case of 4-points bending test: only the central portion of the beam, that is the one object to the highest (and constant) bending moment, is made of lattice. The sample, corresponding to this middle region, is placed between two supporting ends, made of bulk material. The reason for this solution is that it loads the sample at the highest bending moment. The two ends are just necessary for letting the moment grow from zero (at external constraints) to its maximum, which coincides with the point where the shear forces are applied. This is also advantageous from the point of view of the eventual manufacturing of the sample: since printing lattice is expensive and time consuming, it is useless to print them in section of the sample where there is no interest in their behavior. Dimensions and geometry of the sample can be found in Fig. 1. The material considered for this investigation is AISI 316 stainless steel (E = 200000 MPa, ν = 0.3), and lattice cell used is the all-face-centered-cubic (*afcc*), that can be seen in Fig.1 as well: the diameter of the lattice struts is constant and equal to 0,54 mm, while the edge length of the single representative volume element (RVE) is 3 mm.

First step of the process is the homogenization of the lattice structure: that means defining an orthotropic material that presents equivalent mechanical properties as the single lattice RVE. The process is applied through Ansys Mechanical APDL, where, after the definition of the finite elements model of a whole RVE, it is possible to define a routine via command panel that applies different load cases employed for the extraction of the equivalent mechanical properties. Load cases are six: three for traction, one for each direction, and three for shear, one for each plane; from these six consecutive simulations, Young's moduli, shear moduli and Poisson's ratios are evaluated. The process has been conceived and described in detail by the authors in [13].

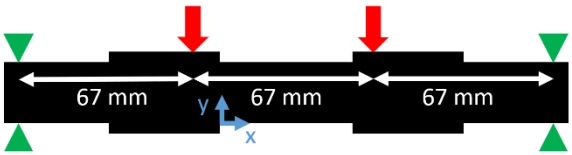

Figure 1: Boundary condition scheme for the simplified model

Once obtained the equivalent properties of the lattice, it is possible use them for the generation of a simplified model where the medium material is used in place of lattice. Every lattice RVE is modeled by a single 8-nodes solid element (in Ansys SOLID185); such elements are employed for the rest of the sample as well, where lattice is not present. The case considered in this investigation for the 4-point bending fatigue test, is a symmetrical load case with static load equal to zero and alternate load equal to 100 N (stress ratio $R = -1$).

Static simulation loads and boundaries applied on the simplified model are schematized in Fig. 2: 100 N distributed force is applied to the central points of the sample (red arrows) and line of nodes of the external points are fixed in the y direction only (green triangles). External and middle points are 67 mm distant each other.

Once performed the analysis, it is possible to evaluate which one is the most critical element, that is supposed to coincide with the lattice cell from where fatigue failure of the sample will start. With this aim, a strain-based criterion is employed: for every element of the medium material representing the lattice, the strain tensor norm $\|\varepsilon\|$ (Eq. 1) is

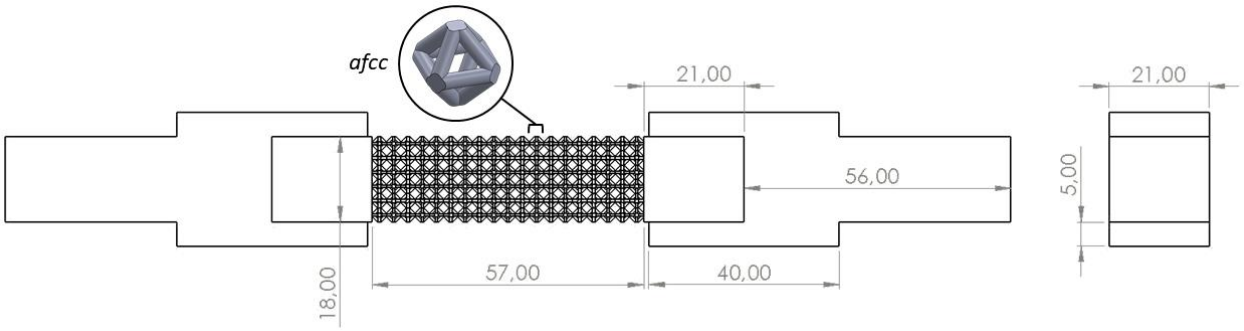

Figure 2: lattice sample and supports with relative dimensions

evaluated. The most critical element is identified with the one presenting the higher $\|\varepsilon\|$.

$$\|\varepsilon\| = \sqrt{\sum_{ij}|\varepsilon_{ij}|^2} \quad for\ i,j = x,y,z \qquad (1)$$

Once the critical element is recognized, it is possible to perform the last step of the method, which is the de-homogenization. Retrieving the strain component of the critical element, it is possible to apply this strain field directly to the actual RVE. In this way, besides being able to retrieve the true stress distribution inside the critical lattice cell and perform a detailed analysis, it is also possible to apply a proper fatigue failure criterion. In this case, being the element analyzed a lattice cell, a tridimensional fatigue failure criterion is chosen: the Crossland criterion. According to this criterion, the fatigue life of a component can be estimated through the expression present in Eq. 2.

$$\tau_{CROSS,eq} = \sqrt{J_{2,a}} + \left(\frac{3\tau_f}{\sigma_f} - \sqrt{3}\right)\sigma_{H,max} \leq \tau_f \qquad (2)$$

The equivalent Crossland stress $\tau_{CROSS,eq}$ is evaluated through shear (τ_f) and bending (σ_f) fatigue limits, the second invariant of the deviatoric stress tensor ($\sqrt{J_{2,a}}$) and the maximum hydrostatic stress ($\sigma_{H,max}$). If the relationship of Eq. 2 is respected, the component presents endless fatigue life.
Results from the method applied to the 4-points bending test will be displayed in the results section.

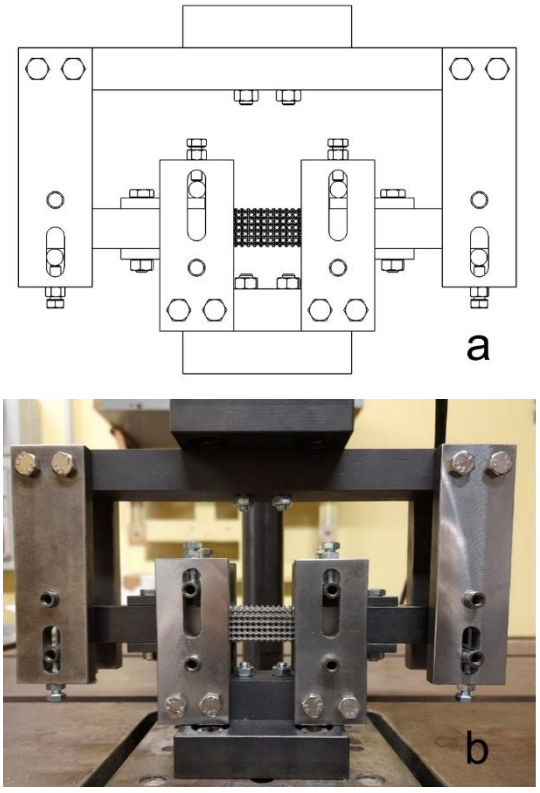

Figure 3: design (a) and mounted on the machine (b) adjuster for 4-points bending fatigue tests

3. EXPERIMENTAL SETUP

An experimental setup for the validation of the model predictions is presented. Machine employed for the application of the fatigue load cycles is the Warner & Swasey Co. fatigue tester SF-1-U: it allows the application of the static load via a hydraulic displacement-control system, while the application of the sinusoidal alternate load is committed to an eccentric mass where it is possible to change the axis of rotation of the mass itself. The load is transmitted to a steel plate. It has been necessary to design a new holding system in order to transform a simple compression-traction load system setup into a 4-point bending one. The scheme of the setup can be seen in Fig. 3a, while the build one in Fig. 3b. All of the components of the adjuster are made of steel.
Sample is held in position on both the upper and lower surfaces on all of the contact points (external and middle) by quenched steel plugs: this is necessary since the lower plate of the machine needs to apply a symmetric alternate cyclic load. with respect to zero. The machine is able to detect the sample breaking, and it stops the eccentric mass from rotating registering the relative number of cycles.

4. RESULTS AND DISCUSSION

Results from the application of the method for the fatigue failure analysis to the 4-points bending test are presented here. First, medium material properties obtained from the homogenization of the *afcc* lattice RVE are shown in Tab. 1.

Table 1: equivalent mechanical properties of the homogenized lattice

$E_X = E_Y = E_Z$	6864 MPa
$G_{XY} = G_{YZ} = G_{XZ}$	3838 MPa
$\nu_{XY} = \nu_{YZ} = \nu_{XZ}$	0.3

The employment of the medium material presents a computational advantage: a smaller number of elements are used, resulting into a lighter model (that for components with a large number of lattice cells is convenient). In addition, the use of elements with the same edge length and of the same type allows a better mesh, instead of modeling a geometry presenting bulk material and

lattice at the same time (that would necessarily require large differences among the elements used).
Fig. 4 shows the distribution of the tensor deformation norm: highest values of this indicator are symmetrically at the bottom and top surfaces of the lattice section

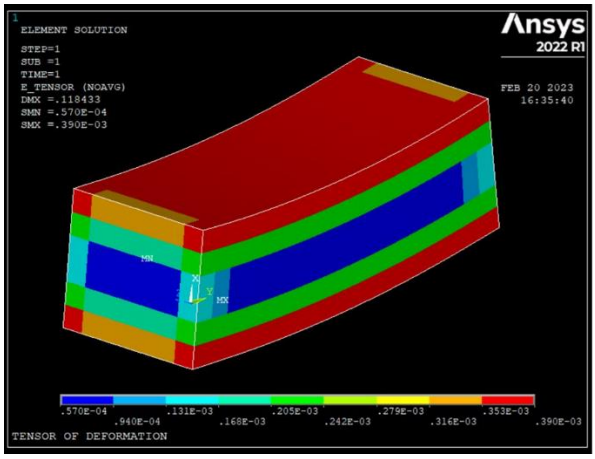

Figure 4: strain tensor norm distribution from the static analysis on the homogenized lattice

The most critical element from the point of view of the strain tensor norm can be found on the lower surface between the middle point and the end of the section (at the middle in the direction of the depth as well), as it can be seen from Fig. 5.

Figure 5: critical element (in green) of the lattice section from the static analysis on the homogenized lattice

Once retrieved the true configuration of the most critical cell through de-homogenization, it has been possible to apply the Crossland fatigue failure criterion. The fringe of the Crossland equivalent stress (Eq. 2) can be seen in Fig.6. The maximum value of such equivalent stress registered in the cell, which is $\tau_{CROSS,eq\ MAX} = 348\ MPa$, is higher than the relative shear fatigue limit of the material, which is $\tau_f = 138\ MPa$. This is the indicator that the lattice presents no endless life by employing the magnitude of 100 N as alternate load.

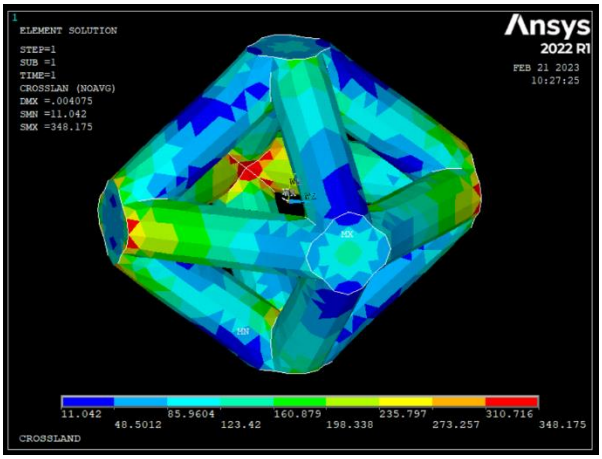

Figure 6: Crossland equivalent stress fringe for the most critical lattice cell

By using other criteria for the evaluation of the fatigue failure, it would be possible to achieve more data about the fatigue life of the sample: an example could be the Sines criterion, together with the drawing of the Haigh diagram.
Due to difficulties encountered with the calibration of the adjuster for the fatigue tester machine, only one sample experimentally tested presents the proper characteristics to be defined as validating for the model. As it can be seen in Fig. 7, the sample is broken at the exact point where the model indicates the presence of the critical element. This sample was loaded at 1800 N of force amplitude. Unfortunately, due to the excessive stiffness of the sample supports, it was not possible to count the exact number of cycles to failure, which is in the range of 3000-5000 cycles. Other samples did not experience fatigue failure: sample 1, with 900 N of force amplitude and sample 2, with 1500 N of force amplitude, have not been experienced failure until 5000000 cycles.

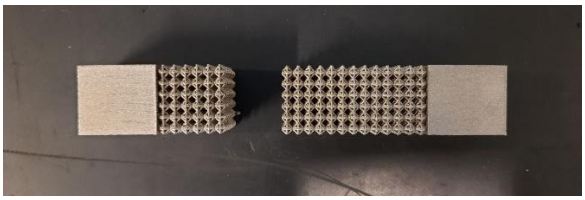

Figure 7: fractured sample from the experimental fatigue test

Some details of the setup still need adjustment: plugs that keep the sample in position need to be locked into the milled slot, since excessive vibrations during tests have made clear that bolts keeping them pressed on the sample are insufficient to guarantee no translation. A lower alternate force would also help reducing vibrations

that could damage the setup. The use of milled slots will be considered to allow the specimen to slide once broken, and therefore allow the machine to properly recognize when to record the number of cycles equivalent to failure. Besides this problem recorded with the setup, the only sample tested properly can be considered as an early validation of the model.

5. CONCLUSIONS

It can be stated that a computationally advantageous method for the fatigue failure analysis of lattice structures has been successfully applied to a 4-points bending test case study. The method offers a simple and lighter process for the recognition of the point from where the fracture that determines the failure of the sample (or eventually component) will start, based on the norm of the strain tensor. The employment of homogenization allows the simulation of large lattice components with a computationally lighter model, while de-homogenization helps performing a detailed analysis of the lattice topology involved. Preliminary experimental results have been observed with no failure and fatigue failure.

6. REFERENCES

1. M. F. Ashby, “Mechanical Properties of Cellular Solids.,” *Metall. Trans. A, Phys. Metall. Mater. Sci.*, vol. 14 A, no. 9, pp. 1755–1769, (1983), doi: 10.1007/BF02645546.
2. V. S. Deshpande, N. A. Fleck, and M. F. Ashby, “Effective properties of the octet-truss lattice material,” *J. Mech. Phys. Solids*, vol. 49, pp. 1747–1769, (2001).
3. A. Seharing, A. H. Azman, and S. Abdullah, “A review on integration of lightweight gradient lattice structures in additive manufacturing parts,” *Adv. Mech. Eng.*, vol. 12, no. 6, pp. 1–21, (2020), doi: 10.1177/1687814020916951.
4. G. De Pasquale and A. Tagliaferri, “Modeling and characterization of mechanical and energetic elastoplastic behavior of lattice structures for aircrafts anti-icing systems,” *Proc. Inst. Mech. Eng. Part C J. Mech. Eng. Sci.*, vol. 235, no. 10, pp. 1828–1839, (2021), doi: 10.1177/0954406219853857.
5. M. Davidson *et al.*, “Investigating amorphous metal composite architectures as spacecraft shielding,” *Adv. Eng. Mater.*, vol. 15, no. 1–2, pp. 27–33, (2013), doi: 10.1002/adem.201200313.
6. Y. Kim, I. Kim, and J. Park, “An approximate formulation for the progressive failure analysis of a composite lattice cylindrical panel in aerospace applications,” *Aerosp. Sci. Technol.*, vol. 106, p. 106212, (2020), doi: 10.1016/j.ast.2020.106212.
7. G. Bianchi, G. S. Aglietti, and G. Richardson, “Static and fatigue behaviour of hexagonal honeycomb cores under in-plane shear loads,” *Appl. Compos. Mater.*, vol. 19, no. 2, pp. 97–115, (2012), doi: 10.1007/s10443-010-9184-5.
8. A. García, F. Sorribes-Palmer, and G. Alonso, “Application of Steinberg vibration fatigue model for structural verification of space instruments,” *AIP Conf. Proc.*, vol. 1922, no. January, (2018), doi: 10.1063/1.5019088.
9. M. Gavazzoni, S. Beretta, and S. Foletti, “Response of an aluminium Schwarz triply periodic minimal surface lattice structure under constant amplitude and random fatigue,” *Int. J. Fatigue*, vol. 163, no. January, p. 107020, (2022), doi: 10.1016/j.ijfatigue.2022.107020.
10. P. Zhang, D. Z.Zhang, and B. Zhong, “Constitutive and damage modelling of selective laser melted Ti-6Al-4V lattice structure subjected to low cycle fatigue,” *Int. J. Fatigue*, vol. 159, no. November 2021, p. 106800, (2022), doi: 10.1016/j.ijfatigue.2022.106800.
11. A. Cutolo and B. Van Hooreweder, “Fatigue behaviour of diamond based Ti-6Al-4V lattice structures produced by laser powder bed fusion: On the effect of load direction,” *Mater. Today Commun.*, vol. 33, no. September, p. 104661, (2022), doi: 10.1016/j.mtcomm.2022.104661.
12. Y. Li, M. J. Pavier, and H. Coules, “Fatigue properties of aluminium triangular lattice plates,” *Procedia Struct. Integr.*, vol. 28, no. 2019, pp. 1148–1159, (2020), doi: 10.1016/j.prostr.2020.11.096.
13. G. De Pasquale and A. Coluccia, “Fatigue failure prediction in lattice structures through numerical method based on de-homogenization process,” *Procedia Struct. Integr.*, vol. 41, pp. 535–543, (2022), doi: 10.1016/j.prostr.2022.05.061.